HHS Public Access

Author manuscript

Dev Neurosci. Author manuscript; available in PMC 2019 September 08.

Published in final edited form as:

Dev Neurosci. 2019 ; 41(1-2): 17–33. doi:10.1159/000496602.

Hypoxia-Ischemia and Hypothermia Independently and Interactively Affect Neuronal Pathology in Neonatal Piglets with Short-Term Recovery

Caitlin E. O'Brien[a], **Polan T. Santos**[a], **Ewa Kulikowicz**[a], **Michael Reyes**[a], **Raymond C. Koehler**[a], **Lee J. Martin**[b,c], **Jennifer K. Lee**[a,c]

[a] Department of Anesthesiology and Critical Care Medicine, Johns Hopkins University, Baltimore, MD, USA

[b] Department of Pathology, Johns Hopkins University, Baltimore, MD, USA

[c] Pathobiology Graduate Training Program, Johns Hopkins University, Baltimore, MD, USA

Abstract

Therapeutic hypothermia is the standard of clinical care for moderate neonatal hypoxic-ischemic encephalopathy. We investigated the independent and interactive effects of hypoxia-ischemia (HI) and temperature on neuronal survival and injury in basal ganglia and cerebral cortex in neonatal piglets. Male piglets were randomized to receive HI injury or sham procedure followed by 29 h of normothermia, sustained hypothermia induced at 2 h, or hypothermia with rewarming during fentanyl-nitrous oxide anesthesia. Viable and injured neurons and apoptotic profiles were counted in the anterior and posterior putamen and in the motor cortex at 29 h after HI injury or sham procedure. Terminal deoxynucleotidyl transferase dUTP nick-end labeling (TUNEL) identified genomic DNA fragmentation to confirm cell death. Though hypothermia after HI preserved viable neurons in the anterior and posterior putamen, hypothermia prevented neuronal injury in only the anterior putamen. Hypothermia initiated 2 h after injury did not protect against apoptotic cell death in either the putamen or motor cortex, and rewarming from hypothermia was associated with increased apoptosis in the motor cortex. In non-HI shams, sustained hypothermia during anesthesia was associated with neuronal injury and corresponding viable neuron loss in the anterior putamen and motor cortex. TUNEL confirmed increased neurodegeneration in the putamen of hypothermic shams. Anesthetized, normothermic shams did not show abnormal neuronal cytopathology in the putamen or motor cortex, thereby demonstrating minimal contribution of the anesthetic regimen to neuronal injury during normothermia. We conclude that the efficacy of hypothermic protection after HI is region specific and that hypothermia during anesthesia in the absence of HI may be associated with neuronal injury in the developing brain.

Corresponding author Caitlin O'Brien, MD, MPH, Department of Anesthesiology and Critical Care Medicine, Johns Hopkins University, 1800 Orleans Street, Bloomberg Tower, Suite 6349J, Baltimore, MD 21287 (USA), cobrie19@jhmi.edu.

Disclosure Statement

The authors declare no conflicts of interest.

Statement of Ethics

Animal experiments conform to internationally accepted standards and have been approved by the appropriate institutional review body.

Studies examining the potential interactions between hypothermia and anesthesia, as well as with longer durations of hypothermia, are needed.

Keywords

Neonatal; Brain injury; Hypothermia therapy; Neurodegeneration; Neuroprotection; Hypoxic-ischemic encephalopathy; Perinatal asphyxia

Introduction

Therapeutic hypothermia has been the standard of clinical care for moderate-to-severe hypoxic-ischemic encephalopathy (HIE) in newborns for many years [1]. As clinicians become more comfortable with delivering hypothermia, considerations for its use have expanded to include babies with mild HIE [2–5]. The effects of temperature manipulation independent of hypoxia-ischemia (HI) on the developing brain must be studied as hypothermia is also considered for more diverse patient populations [6]. In some clinical situations, rewarming a neonate who inadvertently becomes hypothermic is essential for safety, including very low birthweight newborns [7] and in the perioperative period [8]. Therefore, we studied independent and interactive effects of HI and temperature management on the developing brain.

We previously demonstrated that hypothermia preserved neuronal viability and reduced ischemic necrosis [9, 10] in a swine model of severe hypoxic-asphyxic brain injury manifesting in part as 80% loss of viable neurons in the putamen [11–14]. Here, we examined the independent and interactive effects of moderate HI and normothermia, sustained hypothermia, and hypothermia with rewarming in piglets that had lesser HI injury or that underwent sham procedure. We studied the neuropathology in the basal ganglia and cerebral cortex because these regions are known to be vulnerable both in our model [13, 15] and in human newborns with HIE [16]. Further, injury in these regions is associated with poor neurodevelopmental outcome [17, 18].

Materials and Methods

Animal Preparation

All procedures were approved by the Animal Care and Use Committee at Johns Hopkins University and complied with the United States Public Health Service Policy on the Humane Care and Use of Laboratory Animals and the Guide for the Care and Use of Laboratory Animals. Animal care ensured comfort and was in accordance with the National Institutes of Health Guidelines. To conserve animals, we analyzed the putamen and motor cortex from brains of piglets that we previously reported in studies of cerebral cortical and white matter injury and the unfolded protein response [15, 19, 20]. Twenty-four additional piglets were used for this study for Western blots. Neonatal male piglets (1–2.5 kg, 2–3 days old) were randomized to sham procedure or HI injury followed by 29 h of normothermia, sustained hypothermia beginning at 2 h after injury or time equivalent, or hypothermia with

rewarming. Age-matched, male, naïve piglets that did not receive anesthesia, surgery, or HI were prepared as an additional control group.

We previously published our HI protocol [15, 19]. Briefly, piglets were anesthetized via nose cone with 5% isoflurane in a 50/50% nitrous oxide/oxygen mixture. After intubation, mechanical ventilation was initiated to maintain normocapnia and normoxia. The inhaled oxygen was decreased to 30% in a 70/30% nitrous oxide/oxygen mixture, and the isoflurane was decreased to 2%. The femoral vein and artery were cannulated for intravenous (IV) administration of 5% dextrose in normal saline (4 mL/kg/h) and fentanyl (20 μg bolus followed by 20 μg/kg/h), as well as continuous arterial blood pressure monitoring. The isoflurane was discontinued after placement of the femoral cannulae, which takes an average of 10–15 min, and initiation of the fentanyl infusion. All piglets received IV vecuronium (0.2 mg/kg/h) to prevent shivering during hypothermia and to provide a consistent anesthetic to all piglets. This anesthetic regimen does not affect white matter apoptosis [19], cortical apoptosis [15], the unfolded protein response [20], or brain proteasomes [21] in our model. Phenylephrine or dopamine was initiated when necessary to maintain the mean arterial blood pressure above 45 mm Hg, which is the lower limit of autoregulation in neonatal swine [22].

Systemic HI Injury

We induced whole-body hypoxia by decreasing the inhaled oxygen to 10% for 45 min to achieve an oxyhemoglobin saturation of 30–35%. The piglets then received room air for 5 min. This brief reoxygenation period is required for cardiac resuscitation. We occluded the endotracheal tube for 7 min to produce asphyxia. Piglets were resuscitated with 50% oxygen, manual chest compressions, and IV epinephrine (100 μg/kg) [23]. Piglets that did not exhibit return of spontaneous circulation (ROSC) within 3 min were excluded. After resuscitation, the inhaled oxygen was decreased to 30% for the remainder of the experiment. Sodium bicarbonate and calcium chloride were administered to correct metabolic acidosis and hypocalcemia, as necessary. Sham-operated piglets received the same femoral cannulae, duration of anesthesia, and 30% inhaled oxygen without HI injury.

Temperature Management

In addition to being randomized to HI or sham procedure, piglets were also randomized to one of three temperature treatments: (1) normothermic for swine), (2) hypothermia (34.0°C) beginning 2 h after ROSC or time equivalent in sham groups, or (3) hypothermia with rewarming at 0.5°C/h, which is the clinical rewarming rate for HIE [1, 24]. We used heating lamps and warming blankets to maintain normothermia or cooling blankets and ice packs to induce and maintain whole-body hypothermia. We delayed the induction of hypothermia by 2 h to mimic clinical delays. The 34.0°C target for hypothermia approximates the 4°C decrease achieved in clinical therapeutic hypothermia (37°C human normothermia with cooling to approximately 33.5 ± 0.5°C) [1, 24, 25]. In our model, rectal temperature decreases to 34°C over 30 min, and rectal and brain temperatures correlate within 0.2°C [10]. We initiated rewarming at 20 h after ROSC (after 18 h of hypothermia) by incrementally increasing the water temperature circulating through the blanket and by the use of heating lamps. Temperature management throughout the procedure was carefully monitored to avoid overcooling during hypothermia or hyperthermic overshoot during

rewarming. The assigned temperature treatment was provided during 29 h of anesthesia, after which the animals were euthanized for histologic and biochemical measurements. This time point was selected because it correlates with observed maximal putamen injury [13, 14].

Histology

At 29 h after ROSC or time equivalent after sham procedure, piglets were deeply anesthetized with 50 mg/kg pentobarbital and transcardially perfused with cold phosphate-buffered saline followed by 4–6 L of ice-cold 4% paraformaldehyde for brain fixation. The brain was stored overnight at 4°C for in situ fixation. Afterwards, we gently removed the brain from the skull, avoiding any instrument and brain handling compression of tissue, cut it midsagittally, and immersed the right hemisphere in 4% paraformaldehyde for postfixation. The hemisphere was cut into 1 cm slabs that were embedded in paraffin and cut into 10-μm coronal sections.

We analyzed anterior putamen at the striatal anatomic level and posterior putamen and motor cortex at the hippocampal anatomic level in one hemisphere with hematoxylin and eosin (H&E) stain. Two investigators (C.E.O. and J.K.L.) counted viable neurons, injured neurons, and apoptotic profiles in putamen by light microscopy at 400× magnification in a total of 10–12 non-overlapping fields of 196 μm^2 per piglet. Cell counts were also conducted in cortical layers 2 and 3 of the entire motor gyrus at 400× magnification. These cortical layers were reliably identified [14, 26]. Counter reliability was screened for accuracy by a third investigator (L.J.M.). In addition, 2 investigators (C.E.O. and J.K.L.) counted viable neurons and apoptotic profiles in the putamen in a random sample of piglets to test interrater reliability. Different microscope fields were counted within each pig for the interrater reliability assessments.

Viable neurons were defined as having a round or oval cell body (generally 8–10 μm in diameter); open nucleus with visible chromatin strands within a diffuse nucleoplasmic matrix, often with a nucleolus; uninterrupted nuclear and cell membranes; normal thin rim of cytoplasm; and no apoptotic or ischemic morphology [15]. Apoptotic profiles were identified as cells with a few (<4) crescent-shaped or spherical chromatin clumps in the nucleus, cytoplasmic condensation, and shrinkage into a round cell body profile with eosinophilic cytoplasm and intact cell membranes [27]. Most apoptotic profiles were at definite end-stage or near end-stage, so the specific cell identity could not be determined. We did not count apoptotic profiles that were adjacent to or within 1 cell diameter of a blood vessel to exclude apoptotic white blood cells, pericytes, or endothelial cells.

We classified injured neurons based on their neuronal morphology as either (1) classical ischemic necrotic cytopathology [23] or (2) eosinophilic cytoplasm with cytoplasmic vacuoles and darkened nucleoplasm, but without overt loss of the nucleoli or other signs of chromatin fragmentation and nuclear disintegration. Classical ischemic necrosis was defined by a shrunken, acutely angular cell body with homogeneous glassy, eosinophilic cytoplasm that contained microvacuoles, but no perinuclear pallor, and a hematoxylin-stained pyknotic, attritional, angular nucleus with dark speckling of the nucleoplasmic matrix and no nucleolus [14, 23]. Neurons with necrotic morphology that included nuclear pyknosis and

eosinophilic, vacuolated cytoplasm were included in the injured neuron counts [15, 28]. Representative images of viable, injured, and apoptotic profiles in the anterior and posterior putamen are shown in Figure 1a–e. Figure 2a–c shows examples of cortical pathology and neuronal classification.

We verified cell death using nuclear terminal deoxynucleotidyl transferase dUTP nick-end labeling (TUNEL) with the In-Situ Cell Death Detection Kit, POD (Roche Applied Science; Penzberg, Germany) as previously described [15]. Slides were developed with 3,3′-diaminobenzidine substrate and counterstained with cresyl violet. Negative controls were not exposed to terminal deoxynucleotidyl transferase, and positive controls were treated with DNase. One investigator (C.E.O.), who was masked to treatment group, counted TUNEL+ profiles. A representative TUNEL+ profile is shown in Figure 1f. We excluded TUNEL+ cells within or adjacent to blood vessels to avoid counting TUNEL+ blood-borne or endothelial cells.

Immunoblotting

These experiments were done to quantify various proteins involved in cell death, inflammation, and the unfolded protein response. All experiments were performed at 29 h after ROSC or time equivalent after sham procedure. Piglets were deeply anesthetized with 50 mg/kg pentobarbital and transcardially perfused with cold phosphate-buffered saline to harvest fresh brain tissue. Putamen was dissected from fresh brain slabs on dry ice. To conserve animals, we analyzed putamen tissue from piglets that we previously reported in studies of cortical [15] and white matter injury [19], as well as the unfolded protein response [20].

Brain samples were homogenized in ice-cold RIPA buffer (Cell Signaling Technology; Danvers, MA, USA), protease inhibitor cocktail (Invitrogen; Grand Island, NE, USA), and phosphatase inhibitor (Roche Applied Science; Mannheim, Germany) at a ratio of 1 mL per 0.1 g tissue. After the homogenates were centrifuged at 4°C, protein concentrations in the supernatant were measured with the Pierce BCA protein assay kit (Thermo Scientific; Rockford, IL, USA). Samples were treated with loading buffer, boiled for 5 min, separated by sodium dodecyl sulfate-polyacrylamide gel electrophoresis on 4–12% Tris-glycine gels, and transferred to nitrocellulose membranes. Each gel contained a putamen homogenate sample from each treatment group. After transfer, the membranes were stained with Ponceau S (Sigma Life Science; St. Louis, MO, USA) and imaged for quantification of protein loading. After being washed, the membranes were blocked in 5% nonfat milk for 1 h at room temperature and then incubated overnight with primary antibody in 2% milk at 4°C (Table 1). The membranes were incubated in anti-goat IgG (Jackson ImmunoResearch; West Grove, PA, USA), anti-mouse IgG (Jackson ImmunoResearch), or anti-rabbit IgG (GE Healthcare; Nottingham, UK) diluted 1:3,000 in 2% milk for 2 h at room temperature. The membranes were imaged with enhanced chemiluminescence (Bio-Rad; Hercules, CA, USA) and iBright CL1000 Imaging System (Invitrogen). Immunoreactive band densities were analyzed with MyImageAnalysis version 2.0 (Thermo Fisher Scientific; Waltham, MA, USA). The densities were normalized to Ponceau protein loading control for analysis. The sizes of the proteins of interest were determined using a molecular weight reference ladder

(Precision Plus Protein Standards, BioRad; Hercules, CA, USA). The following immunoreactive bands were measured: neuronal nuclei (NeuN, 46 kD), caspase-3 (25 kD), heat shock protein 70 (70 kD), endoplasmic reticulum to nucleus signaling 1 (ERN1, 110 kD), protein kinase RNA-like endoplasmic reticulum kinase (145 kD), phosphorylated ERN1 (100 kD), tumor necrosis factor alpha (35 kD), fas cell surface death receptor (Fas-CD95, 50 kD), nitrotyrosine (all bands in each lane), and ionized calcium-binding adapter molecule 1 (15 kD).

Sample Size Calculations

Because we had no a priori data for this model, we conducted a power estimate for detecting an effect of hypothermia on viable neurons in the first third of animals. Viable neuron counts in putamen of 3 HI normothermic and 3 HI hypothermic piglets had a difference in means of 17.4 and a within-group SD of 5.4. A sample size of 4 piglets/group would have a power of 0.90 at an alpha level of 0.05.

Statistical Analysis

Analyses were conducted and graphs generated with SigmaPlot (version 11.2, Systat oftware; Chicago, IL, USA) and GraphPad (version 5.00, GraphPad Software; La Jolla, CA, USA). Data are graphed as box plots with interquartile ranges (IQR) and 5–95th percentile whiskers. Interrater reliability for viable neuron and apoptotic profile counts was analyzed with Pearson correlations and Bland-Altman plots. To examine for possible effects of the anesthetic, we compared cell counts from naïve unanesthetized and sham normothermic groups with *t* tests or Mann-Whitney rank sum tests for parametric and nonparametric data, respectively. We used Pearson correlation and Bland-Altman plots to test agreement between apoptotic profiles, as determined by H&E staining, and TUNEL+ profiles in paired (within pig) comparisons. Immunoblot densities were normalized to those of naïve pigs and then analyzed by Friedman repeated measures analysis of ranks with data blocked by gel. Cell counts between piglets that did or did not receive phenylephrine were compared by Mann-Whitney rank sum tests.

To evaluate the effects of HI and temperature, we assessed the data distribution using the Shapiro-Wilk normality test. We transformed non-normal data by using a log(x+1) function to generate normally distributed data. If this method did not generate a normal distribution, we used an arctan(x) function to achieve normality. We used 2-way analysis of variance to analyze the effects of HI, temperature, and their interactions on viable neuron, apoptotic profile, injured neuron, and TUNEL+ profile counts. Post hoc multiple comparisons were conducted with Holm-Sidak tests.

Results

Treatment Groups and Sizes

Anatomical level-matched sections from 6 naïve, 8 sham normothermia, 7 sham hypothermia, 7 sham rewarming, 6 HI normothermia, 8 HI hypothermia, and 8 HI rewarming piglets (50 total) were used for histologic assessment [15, 19]. Motor cortex was analyzed in the same anatomic level as the posterior putamen. Several slides were not

available for analysis and are described in Appendix 1. We analyzed western blots using tissue from 23 piglets that were part of prior studies [15, 19, 20], and we analyzed putamen tissue from 24 new piglets.

Physiology

We reported blood gas and physiologic data, including the piglets' temperature, pH, $PaCO_2$, mean arterial blood pressure, hemoglobin, and sodium levels, in our prior studies [15, 19]. We provide a summary of select parameters during the HI protocol here for the piglets from which we collected histologic data. Hypoxia caused the mean oxyhemoglobin saturation to decrease to 26 ± 8% in the normothermic group, 30 ± 9% in the hypothermic group, and 27 ± 6% in the rewarmed group. Asphyxia further decreased the oxyhemoglobin saturation to 3 ± 1% in normothermic, 6 ± 3% in hypothermic, and 5 ± 4% in rewarmed piglets. Mean arterial pressure at end-asphyxia ranged from 42 to 52 mm Hg. This blood pressure was higher than that in our previous severe HI model, in which mean arterial pressure was 18–25 mm Hg [10, 29]. Thus, piglets in the current study had less severe HI. Rectal temperatures were maintained at approximately 34°C during hypothermia and were achieved by 30 min into hypothermia. During rewarming, piglets were successfully rewarmed to 38–39°C without exceeding the goal temperature.

Interrater Reliability

In a random sample of 15 piglets, 2 investigators (C.E.O. and J.K.L.) counted 10–12 different microscopic fields in putamen and had significant correlation in viable neuron and apoptotic profile counts (Fig. 3a, c). Identification of apoptotic profiles had low bias between the investigators (Fig. 3d). Viable neuron counts had higher bias (Fig. 3b).

Effect of the Anesthetic

The number of viable neurons in anterior putamen was similar in naïve unanesthetized (n = 5) and sham normothermic (n = 8) piglets (p = 0.693; Fig. 4a). Naïve piglets had more apoptosis in anterior putamen than did sham piglets, with a difference in medians of 0.75 apoptotic profiles per microscope field (196 μm^2) between groups (p = 0.019; Fig. 4b). Both naïve and sham piglets had median injured neuron counts of 0 (IQR for naïve: 0–0.1; IQR for sham: 0–0; p = 0.524).

Naïve (n = 6) and sham normothermic (n = 8) piglets exhibited similar numbers of viable neurons (p = 0.311) and apoptotic profiles (p = 1.00) in posterior putamen (Fig. 4c, d). Median injured neuron counts were 2.1 (IQR 0.2–3.7) in naïve and 0.6 (IQR 0.2–2.6) in sham piglets (p = 0.755).

There were no differences in viable neuron or apoptotic profile counts in the motor cortex in naïve (n = 6) or sham normothermic (n = 8) piglets (p = 0.852 for viable and p = 0.651 for apoptotic counts; Fig. 4e, f). Median injured neuron counts were 0 (IQR 0–0) in naïve and 0 (IQR 0–0) in sham piglets (p = 0.955). Therefore, the fentanyl-nitrous oxide anesthetic did not increase apoptosis above the normal developmental level observed in naïve unanesthetized piglets, and it had minimal effect on the number of viable or injured neurons.

Effects of HI and Temperature on Cell Death

Anterior Putamen—Absolute cell counts in the putamen for each experimental group are presented in Table 2. In the anterior putamen, HI and temperature significantly interacted in their effects on the number of viable neurons ($p < 0.001$; Fig. 5a). HI ($p = 0.668$) and temperature ($p = 0.168$) did not individually affect viable neuron counts. In post hoc pairwise comparisons, HI followed by normothermia decreased the number of viable neurons to below that of HI hypothermia ($p < 0.001$) and HI rewarming ($p < 0.001$). Among sham piglets, both sustained hypothermia ($p < 0.001$) and hypothermia with rewarming ($p = 0.019$) decreased viable neuron counts to below that of sham normothermia. Comparisons between the normothermic groups showed a decrease in the number of viable neurons in HI pigs to below that of shams ($p < 0.001$). After sustained hypothermia, shams had fewer viable neurons than HI pigs ($p < 0.001$). Finally, sham rewarmed pigs had fewer viable neurons than HI rewarmed pigs ($p = 0.038$).

HI independently affected the number of apoptotic profiles in the anterior putamen ($p = 0.004$) and HI and temperature significantly interacted ($p = 0.003$; Fig. 5b). Cooling alone did not have an independent effect ($p = 0.088$). Post hoc comparisons among sham piglets showed that sustained hypothermia increased apoptosis above that of hypothermia with rewarming ($p = 0.002$) or normothermia ($p = 0.002$). During normothermia, HI increased apoptosis above that of sham procedure ($p = 0.010$). HI piglets that were rewarmed from hypothermia also had more apoptosis than rewarmed shams ($p < 0.001$).

The majority of injured neurons in the anterior putamen of HI piglets had classical ischemic necrotic morphology. HI ($p = 0.620$) and temperature ($p = 0.334$) did not independently affect neuronal injury but did significantly interact in their effect on the number of injured neurons ($p < 0.001$; Fig. 5c). After HI, normothermic pigs had more injured neurons than did pigs with sustained hypothermia ($p = 0.003$). Sham piglets with sustained hypothermia ($p = 0.017$) and hypothermia with rewarming ($p = 0.007$) had increased neurodegeneration above that of normothermic shams. Normothermic HI pigs had more injured neurons than did sham pigs ($p = 0.001$). Finally, when comparing piglets that underwent sustained hypothermia, shams had more neuronal degeneration than did HI pigs ($p = 0.008$).

TUNEL staining in the anterior putamen confirmed some of the trends we observed by H&E stain. Temperature and HI interacted in their effect on the number of TUNEL+ cells ($p = 0.035$; Fig. 6a). HI ($p = 0.161$) and temperature ($p = 0.845$) did not independently affect these counts. In post hoc pairwise comparisons, hypothermic shams had more TUNEL+ profiles than did normothermic shams ($p = 0.033$) and rewarmed shams ($p = 0.014$). Shams had more cells with DNA fragmentation than did HI piglets during hypothermia ($p = 0.024$). Among piglets that had both TUNEL+ and H&E apoptotic profile counts, correlation in classifying apoptosis was significant ($r = 0.65$, $p < 0.0001$), with low bias and high agreement (Fig. 6b, c).

Posterior Putamen—In the posterior putamen, HI and cooling significantly interacted in their effect on the number of viable neurons ($p = 0.003$; Fig. 5d). Independently, HI ($p = 0.322$) and temperature ($p = 0.098$) did not affect viable neuron counts. Similar to our observations in the anterior putamen, HI hypothermia ($p = 0.013$) and HI hypothermia with

rewarming ($p = 0.004$) increased the number of viable neurons to exceed that of HI normothermia. After rewarming, shams had fewer viable neurons than did HI pigs ($p = 0.003$)

HI and temperature interacted in their effect on apoptosis ($p = 0.008$; Fig. 5e). HI ($p = 0.459$) and temperature ($p = 0.655$) did not independently affect apoptosis. HI normothermic pigs had more apoptosis than did sham normothermic pigs ($p = 0.032$). By contrast, sham hypothermic pigs had more apoptosis than HI hypothermic pigs ($p = 0.032$). HI and temperature did not affect the number of injured neurons in the posterior putamen ($p > 0.05$ for all comparisons; Fig. 5f). As in the anterior putamen, the majority of injured neurons in the posterior putamen were morphologically ischemic necrotic.

Findings on TUNEL stain were also consistent with some of our observations on H&E stain in the posterior putamen. Temperature independently affected the number of TUNEL+ cells ($p < 0.001$), and there was an interactive effect of HI and cooling ($p < 0.001$). HI did not independently affect the number of TUNEL+ cells ($p = 0.496$). In post hoc pairwise analyses, HI normothermic pigs had more TUNEL+ profiles than did sham normothermic pigs ($p < 0.001$; Fig. 6d). Conversely, sham hypothermic pigs had more TUNEL+ profiles than did HI hypothermic, sham normothermic, and sham rewarmed pigs ($p < 0.001$ for all). Hypothermia and hypothermia with rewarming after HI was associated with fewer TUNEL+ cells than was normothermic recovery ($p = 0.003$ for both). When both TUNEL and H&E were performed, correlation between TUNEL+ cells and apoptotic profiles was significant ($r = 0.57$, $p < 0.0001$) with low bias and high agreement (Fig. 6e, f).

Motor Cortex—HI injury independently ($p = 0.007$) and interactively with temperature ($p < 0.001$) affected the number of viable cortical neurons in layers 2–3 (Fig. 7a). Temperature alone did not affect the viable neuron count ($p = 0.390$). In post hoc comparisons, HI hypothermic piglets had more viable neurons than did sham hypothermic piglets ($p < 0.001$). Normothermic shams also had more viable neurons than did hypothermic ($p = 0.002$) and rewarmed shams ($p = 0.025$).

HI ($p < 0.001$) and temperature ($p = 0.009$) independently and interactively ($p < 0.001$) affected the number of apoptotic profiles (Fig. 7b). HI hypothermia increased apoptosis above that of sham hypothermia ($p = 0.020$). The combination of HI, hypothermia, and rewarming increased apoptosis to exceed that of sham rewarming ($p < 0.001$), HI hypothermia ($p < 0.001$), and HI normothermia ($p < 0.001$).

Many injured neurons in the motor cortex showed morphologic signs of classical ischemic necrosis, whereas others had cytopathology that was primarily focused in the cytoplasm (eosinophilic cytoplasm with vacuoles) without fulminant nuclear degeneration. We classified both of these cell types as injured for the analysis. The injured neurons with eosinophilic and vacuolated cytoplasm, but without overt nuclear signs of ischemic necrosis, were predominately in sham piglets.

HI ($p < 0.001$) and temperature ($p = 0.014$) independently and interactively ($p < 0.001$) affected injured neuron counts (Fig. 7c). Normothermic HI piglets had more injured neurons

than did normothermic shams ($p = 0.015$). HI hypothermia reduced the number of injured neurons to below that of HI normothermia ($p = 0.003$). However, sham hypothermia ($p < 0.001$) and sham rewarming ($p < 0.001$) increased the number of injured neurons to exceed that of HI piglets with the same temperature treatment. Among the sham groups, sustained hypothermia and hypothermia with rewarming increased the injured neuron count to above that of normothermia ($p < 0.001$ for both).

Protein Markers of Cell Death, Inflammation, and the Unfolded Protein Response in the Putamen

We performed Western blotting for protein markers of neuronal viability, cell death, inflammation, and the unfolded protein response. Among the experimental groups, we found no differences in the expression of NeuN or cleaved capase-3 ($p > 0.05$ for both; online suppl. Fig. 1a, b; for all online supplementary material, see www.karger.com/doi/10.1159/000496602); tumor necrosis factor alpha, CD95, nitrotyrosine, or onized calcium-binding adapter molecule 1 ($p > 0.05$ for all; online suppl. Fig. 2a–d); or heat shock protein 70, ERN1, protein kinase RNAlike endoplasmic reticulum kinase, or phosphorylated ERN1 ($p > 0.05$ for all; online suppl. Fig. 3a–d).

Vasopressors

One piglet (sham rewarm) received dopamine. Five piglets received phenylephrine (2 HI normothermia, 1 HI hypothermia, and 2 HI rewarm). In the anterior putamen, the number of viable neurons ($p = 0.813$), apoptotic profiles ($p = 0.107$), and ischemic neurons ($p = 0.624$) did not differ between pigs that received phenylephrine and those that did not receive vasopressor. Phenylephrine also did not affect the number of viable neurons ($p = 0.927$), apoptotic profiles ($p = 1.000$), or ischemic neurons ($p = 0.599$) in posterior putamen relative to those piglets that did not receive vasopressor. Similarly, in motor cortex, administration of phenylephrine did not affect the number of viable neurons ($p = 0.924$), injured neurons ($p = 0.182$), or apoptotic profiles ($p = 0.507$) compared with piglets that did not receive phenylephrine.

Discussion

We identified several findings relevant to the effects of hypothermia on the moderately HI-injured and uninjured developing brain. After HI, sustained hypothermia and hypothermia with rewarming preserved viable neurons in putamen to exceed that of normothermia, in part by preventing neuronal ischemic necrosis in the anterior putamen. However, hypothermia did not prevent neuronal ischemic necrosis in the posterior putamen nor did it protect against an HI-induced increase in apoptosis in the anterior putamen, posterior putamen, or motor cortex. Cooling and rewarming increased neuronal injury in sham piglets independent of HI in both the putamen and motor cortex. The reduction in viable neuron counts in the anterior putamen and cerebral cortex after sham hypothermia and rewarming further suggests that the degenerating cells were neurons. In these areas, the degree of neuronal degeneration was such that hypothermic shams had lower viable neuron counts than the hypothermic HI pigs. Indeed, sham hypothermia was associated with more apoptosis than HI hypothermia in the posterior putamen. These results were supported by TUNEL assay. Thus, we identify

independent and interactive effects between moderate HI and temperature management in the developing brain that are region specific after 27 h of hypothermia. The potential for regional brain differences suggest that clinical HIE studies should measure injury of specific brain regions [30] in addition to using global injury scores [31].

Our study reveals new information on the regional vulnerability to HI and the therapeutic efficacy and potential off-target effects of targeted temperature management. We found that hypothermia protected the anterior putamen specifically from ischemic necrosis after HI but not the posterior putamen. Though the finding that hypothermia protects the piglet striatum after HI is not new [10], the finding that hypothermic protection from necrotic cell death can vary intra-regionally is new. This outcome is perhaps explained by differences in the metabolism and connectivity of these regions. Metabolic mapping of mitochondrial cytochrome c oxidase (complex IV) demonstrates higher activity in the posterior putamen compared to the anterior putamen [14] (see Fig. 14). Thus, hypothermia might be less effective at protecting brain regions with greater metabolic demands possibly because of a more rapid commitment to cell death prior to the onset of hypothermia at 2 h [13, 23]. Further, an interesting corollary is that the afferent connections of the anterior putamen and posterior putamen differ, particularly regarding corticostriatal connectivity in large animals and primates, including humans [32]. Generally, the entire cerebral cortex maps topographically onto the putamen in a pattern that follows the anterior-posterior axis. Thus, the frontal eye fields, supplementary motor area, premotor area, and primary motor cortices connect more anteriorly in putamen, while primary somatosensory, parietal, and visual cortices connect more with middle and posterior putamen in monkey and human [32]. Tract tracing and diffusion tensor imaging tractography studies in pig are uncommon [26], but our emerging data using cortical injection of lentivirus with genetically encoded fluorescent reporters suggest that piglet corticostriatal and thalamostriatal connectivity is similar to primates (L.J.M., P.T.S., J.K.L., unpublished observations). Another similarity to primates is the anterior-posterior pattern of dopamine receptor binding sites seen in the striatum of living piglets [33], which could also contribute to regional variability. Because the piglet model of neonatal HIE elegantly mimics that seen in human HIE [34], we are poised to more deeply understand the mechanisms of selective vulnerability and the potential effects of targeted temperature management on the immature brain in a clinically relevant animal model.

Although the early form of neuronal death after HIE is ischemic necrosis, delayed neurodegeneration is more consistent with apoptosis and ongoing neuronal death likely contributes to long-term neurologic injury [35, 36]. Though post-ischemic hypothermia suppresses apoptosis in rats [37, 38], hypothermia did not protect against apoptosis after HI in our swine model. Several possibilities could account for this finding. We delayed the induction of hypothermia by 2 h to mimic clinical delays, which may occur during resuscitation after birth injury or while transporting the neonate to a neonatal intensive care unit. We previously found that the essential molecular cascades for apoptosis can be activated within 15 min of excitotoxicity in a neonatal rat model [39]. Delaying hypothermia induction by 2–3 h attenuates the neuroprotection in putamen afforded by immediate hypothermia after piglet HI [40, 41]. Therefore, it is possible that the 2 h delay after injury contributed to the inability to protect against apoptotic cell death. Use of adjuvant therapies

that specifically mitigate apoptosis could be one strategy to improve hypothermic neuroprotection.

Further, the ideal duration of hypothermia after HI is unknown. We studied up to 27 h of hypothermia, which is shorter than clinical hypothermia for treatment of HIE, but similar to that of other neonatal swine models [40–43] and longer than that of rodent models. In an adult swine model of cardiac arrest, 48 h of hypothermia prevented hippocampal apoptosis better than 24 h of hypothermia [44]. Because we did not test different durations of hypothermia, we do not know if longer periods would afford greater protection against apoptosis. We do not extend the duration of hypothermia in our neonatal piglets owing to neurotoxicity from prolonged anesthesia (unpublished data). However, additional studies of different durations of hypothermia are needed. Fetal lamb models that maintain placental support from the mother may improve the ability to study long durations of hypothermia in more depth [45], including in uninjured developing brain. Because HI brain injury can evolve over weeks to months [46], long-term recovery studies in large, neonatal animal models with gyrencephalic brain and HI are necessary.

Rewarming from hypothermia after HI increased apoptosis in the motor cortex [15] but not in the putamen. Rewarming is a high-risk period for complications and ongoing brain injury after HIE because it is associated with seizures [47], greater discontinuity on electroencephalogram [48], dysfunctional cerebrovascular autoregulation [25], and neuroinflammation [43, 45]. Although a fetal sheep model of HIE showed that slow rewarming reduced injury measured by EEG relative to rapid rewarming, the actual rewarming rates may be less important than the duration of hypothermia for neuronal protection [49].

As comfort with delivering therapeutic hypothermia grows, clinical hypothermia has been considered for neonatal diseases beyond moderate-to-severe HIE [2–6, 50]. Moreover, neonates without known brain injury require rewarming if they become inadvertently hypothermic, including low birthweight newborns [7] and neonates who undergo surgery [8]. Hypothermia is also used for neonatal cardiopulmonary bypass during repair of congenital heart defects. Thus, the independent effects of hypothermia and rewarming on the uninjured neonatal brain deserve thorough study.

We identified possible risks to the putamen and motor cortex from hypothermia and rewarming in uninjured developing brain. Neuropathology in the striatum is of considerable concern because of its key role in motor control, sensory-motor integration, learning and cognition, and emotional-social behavior [51]. Sham hypothermia was associated with increased apoptosis and a greater number of TUNEL-positive cells compared with those of sham normothermia and sham rewarming in the anterior putamen. Because we selected only one time point after HI or sham procedure to quantify cell death, the hypothermic piglets received 27 h of hypothermia, whereas the rewarmed piglets received 18 h of hypothermia. It is possible that the additional 9 h at 34°C contributed to the increased apoptosis and suggests that prolonged hypothermia may have detrimental effects. This finding is consistent with our prior work in the subcortical white matter [19].

We also observed cortical neuronal injury in sham piglets that received hypothermia including cytoplasmic vacuolization and eosinophilia (Fig. 2). The fate of these injured cortical neurons is not known, and electron microscopy needs to be performed. The biological basis for the sensitivity of the cerebral cortex to hypothermia merits exploration, but one possibility relates to the birthdate and maturation of these neurons. Layers 2 and 3 of neocortex are among the latest born neurons in primate brain [52] so this relative propinquity to cell cycle exiting and immaturity might impart vulnerability to cooling. However, early birthdate would not explain the vulnerability of the anterior putamen to hypothermia because these neurons are born much earlier than superficial cortical neurons [52, 53]. A surprising aspect of the cortical and anterior putamen vulnerability to hypothermia was its mitigation by HI, thus highlighting the potential interactions of their molecular physiologies.

The mechanisms by which hypothermia may contribute to neurodegeneration in the developing brain are unknown. In the absence of other injury, severe hypothermia is known to promote cell death by increasing production of reactive oxygen species [54], contributing to derangements in mitochondrial bioenergetics [55], and diminishing production of antioxidants [56]. Interestingly, some of these deleterious effects are absent in the presence of hypoxia or other brain injury [54, 57].

It is important to consider the potential combined effects of hypothermia and anesthesia on neuronal cytopathology. Anesthetized shams that received 29 h of normothermia had similar viable, apoptotic, and injured neuronal counts as unanesthetized naïve piglets. Therefore, during normothermia our anesthetic regimen alone did not cause apparent neuronal cytopathology, consistent with prior assessments of this anesthetic by several parameters [15, 19–21]. We chose the combination of fentanyl-nitrous oxide because previous work in newborn lambs demonstrated that this regimen provides anesthesia without decreasing the cerebral metabolic rate of oxygen [58], in contrast to many other anesthetic regimens. Because it is unethical to cool piglets in the absence of anesthesia given the risk of shivering, discomfort, and hemodynamic changes, we cannot comment on the effects of hypothermia without anesthesia. Hypothermia decreases neuronal metabolism [59], and it is possible that the cellular injury we observed is related to a synergistic effect between hypothermia and fentanyl-nitrous oxide. For instance, hypothermia during our anesthetic regimen could lower spontaneous cerebral electrical activity to below that of anesthesia alone. Whether very low electrical activity in these circumstances causes neuronal injury is not known and cannot be deciphered in our study.

Nonetheless, further studies on the interactions between hypothermia and sedation or anesthesia should be considered in the developing brain. Although 3 days of hypothermia in healthy adults rats did not produce adverse neurologic effects [60], experiments must be specifically designed in neonatal brain to elucidate the effects of hypothermia, clinically relevant sedation and anesthetic regimens, and their potential synergistic effects before a similar safety profile can be assumed for neonates. The postnatal developing and adult rodent and nonhuman primate brains have many pronounced differences in ion channel glutamate receptor expression patterns [61, 62], neurotransmitters [51], and cell death [63,

64], including apoptosis. Thus, we recommend additional studies on the independent effects of hypothermia and rewarming on the developing brain.

We used Western blotting in an attempt to validate our histologic measurements in putamen, but the data did not match the histologic cell counts. Our sample sizes exceeded those from our previous study, which showed significant cleaved caspase-3 protein level differences in cortex after HI, hypothermia, and rewarming. However, that was in cerebral cortex where apoptosis is highly concentrated in a major cell-dense layer [15]. The inability to detect differences in levels of proteins involved in cell death, inflammation, or the unfolded protein response might relate to our use of a crude homogenate assay, which incorporates proteins from intrinsic neurons, white matter axons enriched in striatal bundles, glial cells, vascular cells, and blood-borne cells. The cellular resolution that is achieved with microscopy is lost with crude homogenate assays, and microscopic counting is a direct one-to-one metric. Furthermore, we assessed protein levels at a single time point which might not reflect upstream mechanisms activated shortly after HI injury.

Our study had several limitations. Although sufficiently powered for histologic outcomes, we used a small sample size and multiple treatment groups. Thus, our results must be replicated in other studies for further interpretation. Interrater reliability analyses showed higher bias for viable neuron counts than for apoptotic profile counts. The differences in viable neuron counts between the 2 investigators who conducted the microscopy are likely due to the different microscope fields that were counted in each pig. We could not ensure that the same microscope field was counted by each investigator. We examined only male piglets. Rodent studies suggest that males may preferentially activate caspase-independent cell death, whereas females may activate caspase-dependent cell death and may be more resistant to HI [65, 66]. The effects of sex on cell death after hypothermia and rewarming with and without HI merits study. Although we believe this model to be a moderate HI injury, we did not perform neurologic assessments and cannot comment on the long-term ramifications of this degree of neuronal loss. We have shown that although most cell death occurs before 24 h in the putamen, it does progress over 96 h in more severe models [13]. Whether moderate HI prolongs the delay in cell death in the putamen or cerebral cortex is unknown. The current standard of care for neonatal HIE is 72 h of hypothermia [1]. We only provided up to 27 h of hypothermia in this study. Longer experiments are necessary to more fully describe the effects of hypothermia on the developing brain. Clinically, neonates are not exposed to 29 h of general anesthesia with nitrous oxide during hypothermia and rewarming as the piglets were in our experiments. We utilize our specific anesthetic regimen to ensure animal comfort.

Conclusion

Hypothermia and hypothermia with rewarming after moderate HI preserved viable neurons in the putamen and protected against neuronal injury in the anterior putamen in neonatal swine. Hypothermia after HI did not prevent neuronal injury in the posterior putamen. Moreover, hypothermia initiated 2 h after injury did not protect against apoptotic cell death in either the putamen or motor cortex, and rewarming from hypothermia was associated with increased apoptosis in motor cortex. After sham procedure, hypothermia was associated with

increased neuronal injury in the anterior putamen and motor cortex with a congruent decrease in the number of viable neurons. The neuronal injury in the cortex was morphologically distinct from that in the putamen. Thus, HI and temperature have independent and interactive effects on neuronal pathology in this neonatal swine model. These effects may be region specific and likely involve different cell death mechanisms that warrant further study.

Supplementary Material

Refer to Web version on PubMed Central for supplementary material.

Acknowledgments

We are grateful to Claire Levine, MS, ELS, for her editorial assistance.

Funding Sources

This work was supported by NIH grants T32HL125239 (C.E.O.), K08NS080984 (J.K.L.), R01 NS107417 (J.K.L.), R01 NS060703 (R.C.K. and L.J.M.), R21 NS095036 (R.C.K.), R01 HL139543 (R.C.K.), and AG05146 (L.J.M.); BrightFocus Foundation A2015332S (L.J.M.); and the American Heart Association Transformational Project Award (J.K.L.).

1: Appendix

Piglets That were Not Analyzed by Histology

We used tissue from our past studies on cortical and white matter injury [15, 19]. For the current study, H&E cell counts could not be conducted in the anterior putamen of one naïve pig and one HI hypothermia pig, and in the posterior putamen of one sham hypothermia pig because tissue at the appropriate anatomic level was unavailable. TUNEL-stained slides from the anterior putamen were not available for one sham normothermia, one sham hypothermia, and one HI normothermia piglet because of tissue damage or incomplete stain. TUNEL-stained slides were not available for two HI normothermia piglets and one HI rewarming piglet in the posterior putamen because of tissue damage.

References

1. Shankaran S, Laptook AR, Ehrenkranz RA, Tyson JE, McDonald SA, Donovan EF, et al.; National Institute of Child Health and Human Development Neonatal Research Network. Whole-body hypothermia for neonates with hypoxic-ischemic encephalopathy. N Engl J Med. 2005 10;353(15): 1574–84. [PubMed: 16221780]
2. Lodygensky GA, Battin MR, Gunn AJ. Mild neonatal encephalopathy-how, when, and how much to treat? JAMA Pediatr. 2018 1;172(1):3–4. [PubMed: 29114743]
3. Kracer B, Hintz SR, Van Meurs KP, Lee HC. Hypothermia therapy for neonatal hypoxic ischemic encephalopathy in the state of California. J Pediatr. 2014 8;165(2):267–73. [PubMed: 24929331]
4. Azzopardi D, Strohm B, Linsell L, Hobson A, Juszczak E, Kurinczuk JJ, et al.; UK TOBY Cooling Register. Implementation and conduct of therapeutic hypothermia for perinatal asphyxial encephalopathy in the UK—analysis of national data. PLoS One. 2012;7(6):e38504. [PubMed: 22719897]
5. Oliveira V, Singhvi DP, Montaldo P, Lally PJ, Mendoza J, Manerkar S, et al. Therapeutic hypothermia in mild neonatal encephalopathy: a national survey of practice in the UK. Arch Dis Child Fetal Neonatal Ed. 2018 7;103(4):F388–90. [PubMed: 28942433]

6. Hall NJ, Eaton S, Peters MJ, Hiorns MP, Alexander N, Azzopardi DV, et al. Mild controlled hypothermia in preterm neonates with advanced necrotizing enterocolitis. Pediatrics. 2010 2;125(2):e300–8. [PubMed: 20100756]
7. Feldman A, De Benedictis B, Alpan G, La Gamma EF, Kase J. Morbidity and mortality associated with rewarming hypothermic very low birth weight infants. J Neonatal Perinatal Med. 2016 9;9(3): 295–302. [PubMed: 27589554]
8. Engorn BM, Kahntroff SL, Frank KM, Singh S, Harvey HA, Barkulis CT, et al. Perioperative hypothermia in neonatal intensive care unit patients: effectiveness of a thermoregulation intervention and associated risk factors. Paediatr Anaesth. 2017 2;27(2):196–204. [PubMed: 27917566]
9. Zhu J, Wang B, Lee JH, Armstrong JS, Kulikowicz E, Bhalala US, et al. Additive Neuroprotection of a 20-HETE Inhibitor with Delayed Therapeutic Hypothermia after Hypoxia-Ischemia in Neonatal Piglets. Dev Neurosci. 2015;37(4–5):376–89. [PubMed: 25721266]
10. Agnew DM, Koehler RC, Guerguerian AM, Shaffner DH, Traystman RJ, Martin LJ, et al. Hypothermia for 24 hours after asphyxic cardiac arrest in piglets provides striatal neuroprotection that is sustained 10 days after rewarming. Pediatr Res. 2003 8;54(2):253–62. [PubMed: 12736390]
11. Yang ZJ, Torbey M, Li X, Bernardy J, Golden WC, Martin LJ, et al. Dopamine receptor modulation of hypoxic-ischemic neuronal injury in striatum of newborn piglets. J Cereb Blood Flow Metab. 2007 7;27(7):1339–51. [PubMed: 17213860]
12. Martin LJ, Brambrink AM, Price AC, Kaiser A, Agnew DM, Ichord RN, et al. Neuronal death in newborn striatum after hypoxia-ischemia is necrosis and evolves with oxidative stress. Neurobiol Dis. 2000 6;7(3):169–91. [PubMed: 10860783]
13. Martin LJ, Brambrink AM, Lehmann C, Portera-Cailliau C, Koehler R, Rothstein J, et al. Hypoxia-ischemia causes abnormalities in glutamate transporters and death of astroglia and neurons in newborn striatum. Ann Neurol. 1997 9;42(3):335–48. [PubMed: 9307255]
14. Martin LJ, Brambrink A, Koehler RC, Traystman RJ. Primary sensory and forebrain motor systems in the newborn brain are preferentially damaged by hypoxia-ischemia. J Comp Neurol. 1997 1;377(2):262–85. [PubMed: 8986885]
15. Wang B, Armstrong JS, Lee JH, Bhalala U, Kulikowicz E, Zhang H, et al. Rewarming from therapeutic hypothermia induces cortical neuron apoptosis in a swine model of neonatal hypoxic-ischemic encephalopathy. J Cereb Blood Flow Metab. 2015 5;35(5):781–93. [PubMed: 25564240]
16. Huang BY, Castillo M. Hypoxic-ischemic brain injury: imaging findings from birth to adulthood. Radiographics. 2008 Mar-Apr;28(2):417–39. [PubMed: 18349449]
17. Trivedi SB, Vesoulis ZA, Rao R, Liao SM, Shimony JS, McKinstry RC, et al. A validated clinical MRI injury scoring system in neonatal hypoxic-ischemic encephalopathy. Pediatr Radiol. 2017 10;47(11):1491–9. [PubMed: 28623417]
18. Groenendaal F, de Vries LS. Fifty years of brain imaging in neonatal encephalopathy following perinatal asphyxia. Pediatr Res. 2017 1;81(1–2):150–5. [PubMed: 27673422]
19. Wang B, Armstrong JS, Reyes M, Kulikowicz E, Lee JH, Spicer D, et al. White matter apoptosis is increased by delayed hypothermia and rewarming in a neonatal piglet model of hypoxic ischemic encephalopathy. Neuroscience. 2016 3;316:296–310. [PubMed: 26739327]
20. Lee JK, Wang B, Reyes M, Armstrong JS, Kulikowicz E, Santos PT, et al. Hypothermia and Rewarming Activate a Macroglial Unfolded Protein Response Independent of Hypoxic-Ischemic Brain Injury in Neonatal Piglets. Dev Neurosci. 2016;38(4):277–94. [PubMed: 27622292]
21. Santos PT, O'Brien CE, Chen MW, Hopkins CD, Adams S, Kulikowicz E, et al. Proteasome Biology Is Compromised in White Matter After Asphyxic Cardiac Arrest in Neonatal Piglets. J Am Heart Assoc. 2018 10;7(20):e009415. [PubMed: 30371275]
22. Larson AC, Jamrogowicz JL, Kulikowicz E, Wang B, Yang ZJ, Shaffner DH, et al. Cerebrovascular autoregulation after rewarming from hypothermia in a neonatal swine model of asphyxic brain injury. J Appl Physiol (1985). 2013 11;115(10):1433–42. [PubMed: 24009008]
23. Mueller-Burke D, Koehler RC, Martin LJ. Rapid NMDA receptor phosphorylation and oxidative stress precede striatal neurodegeneration after hypoxic ischemia in newborn piglets and are attenuated with hypothermia. Int J Dev Neurosci. 2008 2;26(1):67–76. [PubMed: 17950559]

24. Azzopardi D, Brocklehurst P, Edwards D, Halliday H, Levene M, Thoresen M, et al.; TOBY Study Group. The TOBY Study. Whole body hypothermia for the treatment of perinatal asphyxial encephalopathy: a randomised controlled trial. BMC Pediatr. 2008 4;8(1):17. [PubMed: 18447921]
25. Burton VJ, Gerner G, Cristofalo E, Chung SE, Jennings JM, Parkinson C, et al. A pilot cohort study of cerebral autoregulation and 2-year neurodevelopmental outcomes in neonates with hypoxic-ischemic encephalopathy who received therapeutic hypothermia. BMC Neurol. 2015 10;15(1):209. [PubMed: 26486728]
26. Jelsing J, Hay-Schmidt A, Dyrby T, Hemmingsen R, Uylings HB, Pakkenberg B. The prefrontal cortex in the Göttingen minipig brain defined by neural projection criteria and cytoarchitecture. Brain Res Bull. 2006 10;70(4–6):322–36. [PubMed: 17027768]
27. Northington FJ, Zelaya ME, O'Riordan DP, Blomgren K, Flock DL, Hagberg H, et al. Failure to complete apoptosis following neonatal hypoxia-ischemia manifests as "continuum" phenotype of cell death and occurs with multiple manifestations of mitochondrial dysfunction in rodent forebrain. Neuroscience. 2007 11;149(4):822–33. [PubMed: 17961929]
28. Lee JK, Yang ZJ, Wang B, Larson AC, Jamrogowicz JL, Kulikowicz E, et al. Noninvasive autoregulation monitoring in a swine model of pediatric cardiac arrest. Anesth Analg. 2012 4;114(4):825–36. [PubMed: 22314692]
29. Brambrink AM, Martin LJ, Hanley DF, Becker KJ, Koehler RC, Traystman RJ. Effects of the AMPA receptor antagonist NBQX on outcome of newborn pigs after asphyxic cardiac arrest. J Cereb Blood Flow Metab. 1999 8;19(8):927–38. [PubMed: 10458600]
30. Tekes A, Poretti A, Scheurkogel MM, Huisman TA, Howlett JA, Alqahtani E, et al. Apparent diffusion coefficient scalars correlate with near-infrared spectroscopy markers of cerebrovascular autoregulation in neonates cooled for perinatal hypoxic-ischemic injury. AJNR Am J Neuroradiol. 2015 1;36(1):188–93. [PubMed: 25169927]
31. Carrasco M, Perin J, Jennings JM, Parkinson C, Gilmore MM, Chavez-Valdez R, et al. Cerebral Autoregulation and Conventional and Diffusion Tensor Imaging Magnetic Resonance Imaging in Neonatal Hypoxic-Ischemic Encephalopathy. Pediatr Neurol. 2018 5;82:36–43. [PubMed: 29622488]
32. Neggers SF, Zandbelt BB, Schall MS, Schall JD. Comparative diffusion tractography of corticostriatal motor pathways reveals differences between humans and macaques. J Neurophysiol. 2015 4;113(7):2164–72. [PubMed: 25589589]
33. Rosa-Neto P, Doudet DJ, Cumming P. Gradients of dopamine D1- and D2/3-binding sites in the basal ganglia of pig and monkey measured by PET. Neuroimage. 2004 7;22(3):1076–83. [PubMed: 15219579]
34. Maller AI, Hankins LL, Yeakley JW, Butler IJ. Rolandic type cerebral palsy in children as a pattern of hypoxic-ischemic injury in the full-term neonate. J Child Neurol. 1998 7;13(7):313–21. [PubMed: 9701479]
35. Nakajima W, Ishida A, Lange MS, Gabrielson KL, Wilson MA, Martin LJ, et al. Apoptosis has a prolonged role in the neurodegeneration after hypoxic ischemia in the newborn rat. J Neurosci. 2000 11;20(21):7994–8004. [PubMed: 11050120]
36. Northington FJ, Ferriero DM, Flock DL, Martin LJ. Delayed neurodegeneration in neonatal rat thalamus after hypoxia-ischemia is apoptosis. J Neurosci. 2001 3;21(6):1931–8. [PubMed: 11245678]
37. Xiong M, Cheng GQ, Ma SM, Yang Y, Shao XM, Zhou WH. Post-ischemic hypothermia promotes generation of neural cells and reduces apoptosis by Bcl-2 in the striatum of neonatal rat brain. Neurochem Int. 2011 5;58(6):625–33. [PubMed: 21300124]
38. Fan J, Cai S, Zhong H, Cao L, Hui K, Xu M, et al. Therapeutic hypothermia attenuates global cerebral reperfusion-induced mitochondrial damage by suppressing dynamin-related protein 1 activation and mitochondria-mediated apoptosis in a cardiac arrest rat model. Neurosci Lett. 2017 4;647:45–52. [PubMed: 28242326]
39. Lok J, Martin LJ. Rapid subcellular redistribution of Bax precedes caspase-3 and endonuclease activation during excitotoxic neuronal apoptosis in rat brain. J Neurotrauma. 2002 7;19(7):815–28. [PubMed: 12184852]

40. Karlsson M, Tooley JR, Satas S, Hobbs CE, Chakkarapani E, Stone J, et al. Delayed hypothermia as selective head cooling or whole body cooling does not protect brain or body in newborn pig subjected to hypoxia-ischemia. Pediatr Res. 2008 7;64(1):74–8. [PubMed: 18391848]
41. Tooley JR, Satas S, Porter H, Silver IA, Thoresen M. Head cooling with mild systemic hypothermia in anesthetized piglets is neuroprotective. Ann Neurol. 2003 1;53(1):65–72. [PubMed: 12509849]
42. Kerenyi A, Kelen D, Faulkner SD, Bainbridge A, Chandrasekaran M, Cady EB, et al. Systemic effects of whole-body cooling to 35 °C, 33.5 °C, and 30 °C in a piglet model of perinatal asphyxia: implications for therapeutic hypothermia. Pediatr Res. 2012 5;71(5):573–82. [PubMed: 22314664]
43. Rocha-Ferreira E, Kelen D, Faulkner S, Broad KD, Chandrasekaran M, Kerenyi Á, et al. Systemic pro-inflammatory cytokine status following therapeutic hypothermia in a piglet hypoxia-ischemia model. J Neuroinflammation. 2017 3;14(1):44. [PubMed: 28253907]
44. Suh GJ, Kwon WY, Kim KS, Lee HJ, Jeong KY, Jung YS, et al. Prolonged therapeutic hypothermia is more effective in attenuating brain apoptosis in a Swine cardiac arrest model. Crit Care Med. 2014 2;42(2):e132–42. [PubMed: 24145844]
45. Davidson JO, Draghi V, Whitham S, Dhillon SK, Wassink G, Bennet L, et al. How long is sufficient for optimal neuroprotection with cerebral cooling after ischemia in fetal sheep? J Cereb Blood Flow Metab. 2018 6;38(6):1047–59. [PubMed: 28504050]
46. Geddes R, Vannucci RC, Vannucci SJ. Delayed cerebral atrophy following moderate hypoxia-ischemia in the immature rat. Dev Neurosci. 2001;23(3):180–5. [PubMed: 11598317]
47. Birca A, Lortie A, Birca V, Decarie JC, Veilleux A, Gallagher A, et al. Rewarming affects EEG background in term newborns with hypoxic-ischemic encephalopathy undergoing therapeutic hypothermia. Clin Neurophysiol. 2016 4;127(4):2087–94. [PubMed: 26749567]
48. Lee JK, Poretti A, Perin J, Huisman TA, Parkinson C, Chavez-Valdez R, et al. Optimizing cerebral autoregulation may decrease neonatal regional hypoxic-ischemic brain injury. Dev Neurosci. 2017;39(1–4):248–56. [PubMed: 27978510]
49. Davidson JO, Wassink G, Draghi V, Dhillon SK, Bennet L, Gunn AJ. Limited benefit of slow rewarming after cerebral hypothermia for global cerebral ischemia in near-term fetal sheep. J Cereb Blood Flow Metab. 2018 8;X18791631.
50. Lichter-Konecki U, Nadkarni V, Moudgil A, Cook N, Poeschl J, Meyer MT, et al. Feasibility of adjunct therapeutic hypothermia treatment for hyperammonemia and encephalopathy due to urea cycle disorders and organic acidemias. Mol Genet Metab. 2013 8;109(4):354–9. [PubMed: 23791307]
51. Martin LJ, Cork LC. The non-human primate striatum undergoes marked prolonged remodeling during postnatal development. Front Cell Neurosci. 2014 9;8:294. [PubMed: 25294985]
52. Rakic P Evolution of the neocortex: a perspective from developmental biology. Nat Rev Neurosci. 2009 10;10(10):724–35. [PubMed: 19763105]
53. Brand S, Rakic P. Genesis of the primate neostriatum: [3H]thymidine autoradiographic analysis of the time of neuron origin in the rhesus monkey. Neuroscience. 1979;4(6):767–78. [PubMed: 113693]
54. Rauen U, Polzar B, Stephan H, Mannherz HG, de Groot H. Cold-induced apoptosis in cultured hepatocytes and liver endothelial cells: mediation by reactive oxygen species. FASEB J. 1999 1;13(1):155–68. [PubMed: 9872940]
55. Riess ML, Camara AK, Kevin LG, An J, Stowe DF. Reduced reactive O2 species formation and preserved mitochondrial NADH and [Ca2+] levels during short-term 17 degrees C ischemia in intact hearts. Cardiovasc Res. 2004 2;61(3):580–90. [PubMed: 14962488]
56. Dede S, Deger Y, Meral I. Effect of short-term hypothermia on lipid peroxidation and antioxidant enzyme activity in rats. J Vet Med A Physiol Pathol Clin Med. 2002 8;49(6):286–8. [PubMed: 12227469]
57. Alva N, Palomeque J, Carbonell T. Oxidative stress and antioxidant activity in hypothermia and rewarming: can RONS modulate the beneficial effects of therapeutic hypothermia? Oxid Med Cell Longev. 2013;2013:957054. [PubMed: 24363826]

58. Yaster M, Koehler RC, Traystman RJ. Interaction of fentanyl and nitrous oxide on peripheral and cerebral hemodynamics in newborn lambs. Anesthesiology. 1994 2;80(2):364–71. [PubMed: 8311318]

59. Hägerdal M, Harp J, Nilsson L, Siesjö BK. The effect of induced hypothermia upon oxygen consumption in the rat brain. J Neurochem. 1975 2;24(2):311–6. [PubMed: 1113108]

60. Auriat AM, Klahr AC, Silasi G, Maclellan CL, Penner M, Clark DL, et al. Prolonged hypothermia in rat: a safety study using brain-selective and systemic treatments. Ther Hypothermia Temp Manag. 2012 3;2(1):37–43. [PubMed: 24717136]

61. Portera-Cailliau C, Price DL, Martin LJ. N-methyl-D-aspartate receptor proteins NR2A and NR2B are differentially distributed in the developing rat central nervous system as revealed by subunit-specific antibodies. J Neurochem. 1996 2;66(2):692–700. [PubMed: 8592141]

62. Martin LJ, Al-Abdulla NA, Brambrink AM, Kirsch JR, Sieber FE, Portera-Cailliau C. Neurodegeneration in excitotoxicity, global cerebral ischemia, and target deprivation: A perspective on the contributions of apoptosis and necrosis. Brain Res Bull. 1998 7;46(4):281–309. [PubMed: 9671259]

63. Portera-Cailliau C, Price DL, Martin LJ. Excitotoxic neuronal death in the immature brain is an apoptosis-necrosis morphological continuum. J Comp Neurol. 1997 2;378(1):70–87. [PubMed: 9120055]

64. Portera-Cailliau C, Price DL, Martin LJ. Non-NMDA and NMDA receptor-mediated excitotoxic neuronal deaths in adult brain are morphologically distinct: further evidence for an apoptosis-necrosis continuum. J Comp Neurol. 1997 2;378(1):88–104. [PubMed: 9120056]

65. Zhu C, Xu F, Wang X, Shibata M, Uchiyama Y, Blomgren K, et al. Different apoptotic mechanisms are activated in male and female brains after neonatal hypoxia-ischaemia. J Neurochem. 2006 2;96(4):1016–27. [PubMed: 16412092]

66. Hill CA, Alexander ML, McCullough LD, Fitch RH. Inhibition of X-linked inhibitor of apoptosis with embelin differentially affects male versus female behavioral outcome following neonatal hypoxia-ischemia in rats. Dev Neurosci. 2011;33(6):494–504. [PubMed: 22041713]

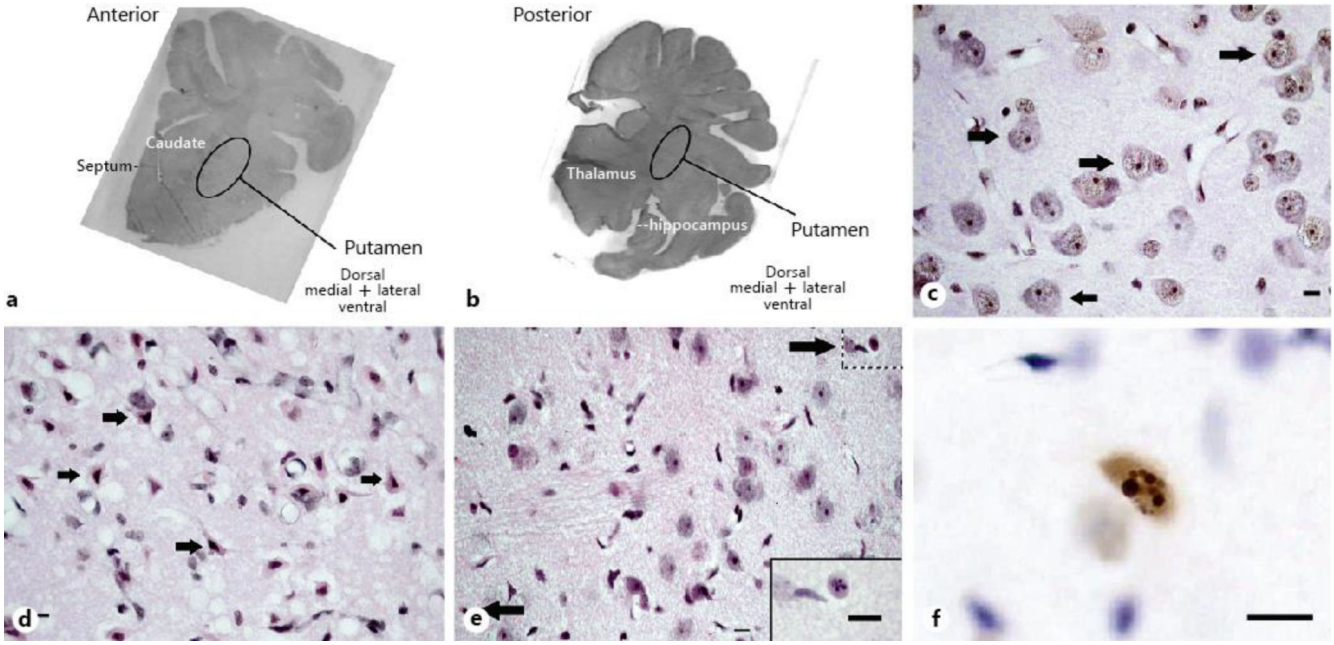

Fig. 1.

Representative brain images from pigs that underwent sham surgery or HI injury. **a**, **b** Macrophotographs show the anterior and posterior levels of the putamen where viable, injured, and apoptotic profiles were counted. Photos are grayscale images of hematoxylin and eosin (H&E)-stained sections that were taken at 10× magnification. Brain section orientation is indicated at the lower right of each image. **c** H&E-stained putamen in a sham-operated normothermic pig. Arrows denote morphologically viable neurons. Perineuronal, pericapillary, and parenchymal neuropil integrity appears excellent at this resolution. **d** H&E-stained putamen in an HI normothermic pig. The arrows identify morphologically ischemic necrotic neurons, which were classified as "injured" for the analysis. Neuropil integrity is severely damaged as evidenced by the overt perineuronal, pericapillary, and parenchymal vacuoles. **e** H&E-stained putamen in a sham-operated hypothermic pig. Arrows denote apoptotic profiles. The neuropil appears finely vacuolated with some pallor. The inset at lower right demonstrates an apoptotic profile at higher magnification (from upper right hatched box) for better visualization of spherical chromatin clumps in the nucleus. **f** Representative TUNEL+ profile in a sham-operated hypothermic pig. The morphology of the DNA fragmentation and compartmentation seen as round aggregates is consistent with apoptosis. The cell size suggests that this apoptotic profile is a neuron. **c**–**d** were taken at 400× magnification. **f** was taken at 600× magnification with oil immersion. Scale bar is 10 μm.

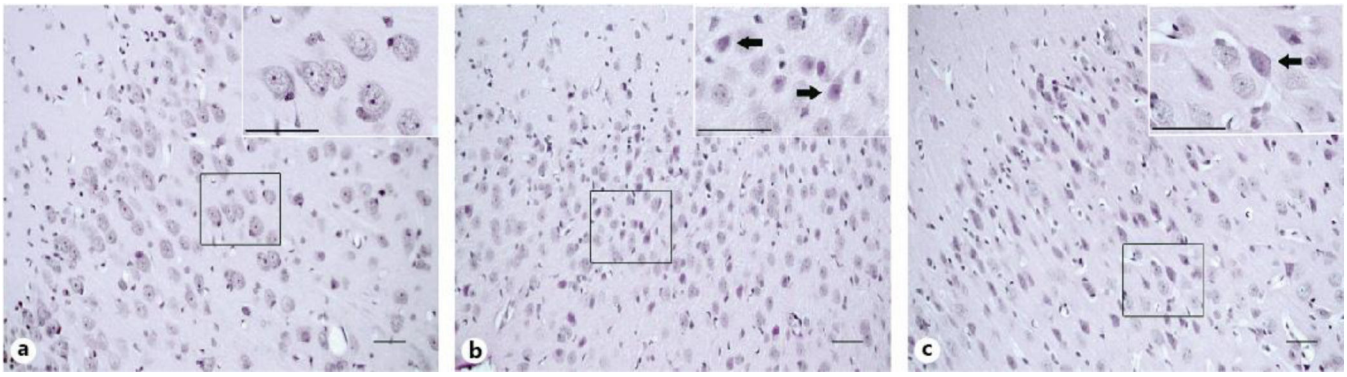

Fig. 2.

Representative hematoxylin and eosin (H&E)-stained sections of motor cortex in pigs that underwent sham surgery and normothermic recovery (**a**), sustained hypothermia (**b**), or hypothermia with rewarming (**c**). Shown are low magnification panoramic and higher resolution (insets) views to appreciate the general anatomic locations and the cellular details. **a** In a sham normothermic piglet, neurons in layers 2 and 3 appear morphologically viable. **b**, **c** After hypothermia and hypothermia with rewarming, subsets of neurons are characterized by vacuolated, eosinophilic cytoplasm and nuclei that are dark and condensed but maintain nucleoli (arrows). The neuropil also shows spongiform changes. Photos taken at 200× magnification and insets taken at 600× magnification. Scale bar is 50 μm.

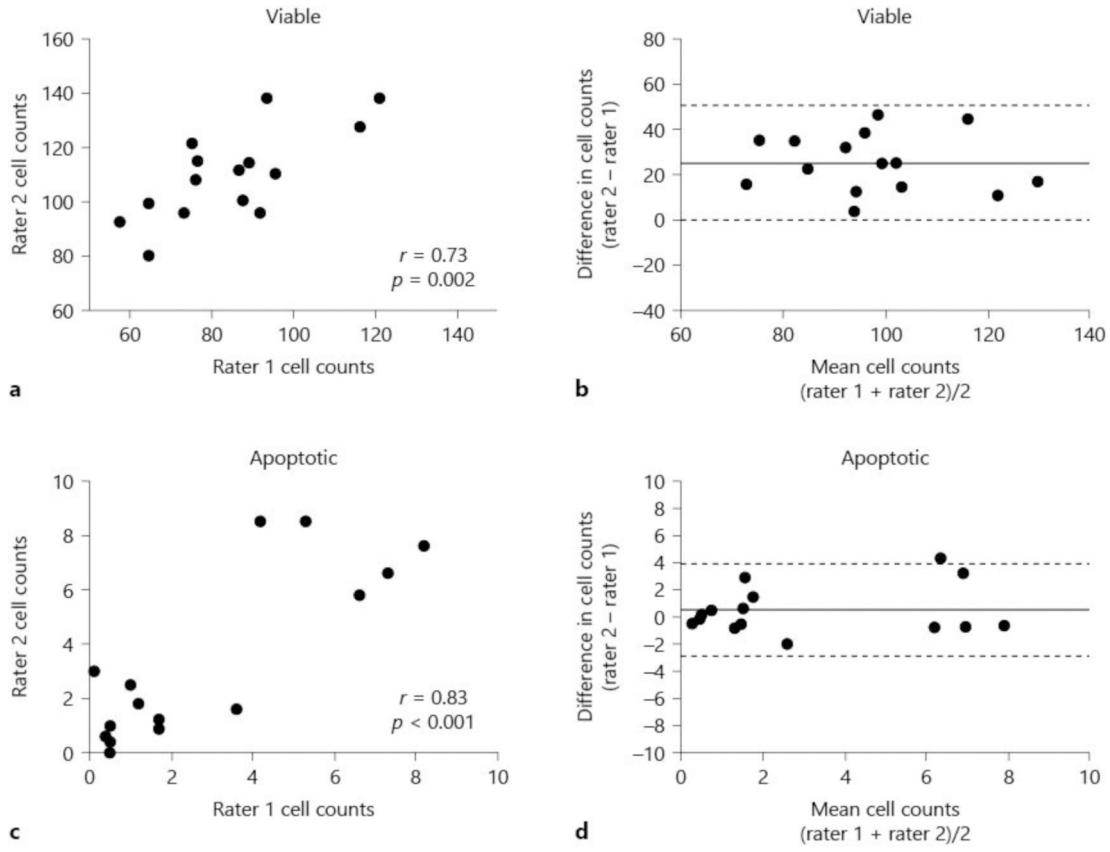

Fig. 3.

Interrater reliability for counting viable neurons (a, b) and apoptotic profiles (**c**, d) on hematoxylin and eosin (H&E)-stained sections in putamen of 15 random piglets. Two investigators counted cells in different microscope fields of the same pig. Viable neuron counts (**a**; $r = 0.73$, $p = 0.002$) and apoptotic profile counts (**c**; $r = 0.83$, $p < 0.001$) correlated between the investigators. Bland-Altman plots for viable neurons (**b**) and apoptotic profiles (**d**). Bias is shown by the solid line. The 95% limits of agreement are shown by dotted lines. The apoptotic counts had near-zero bias, whereas bias was higher for viable neuron counts.

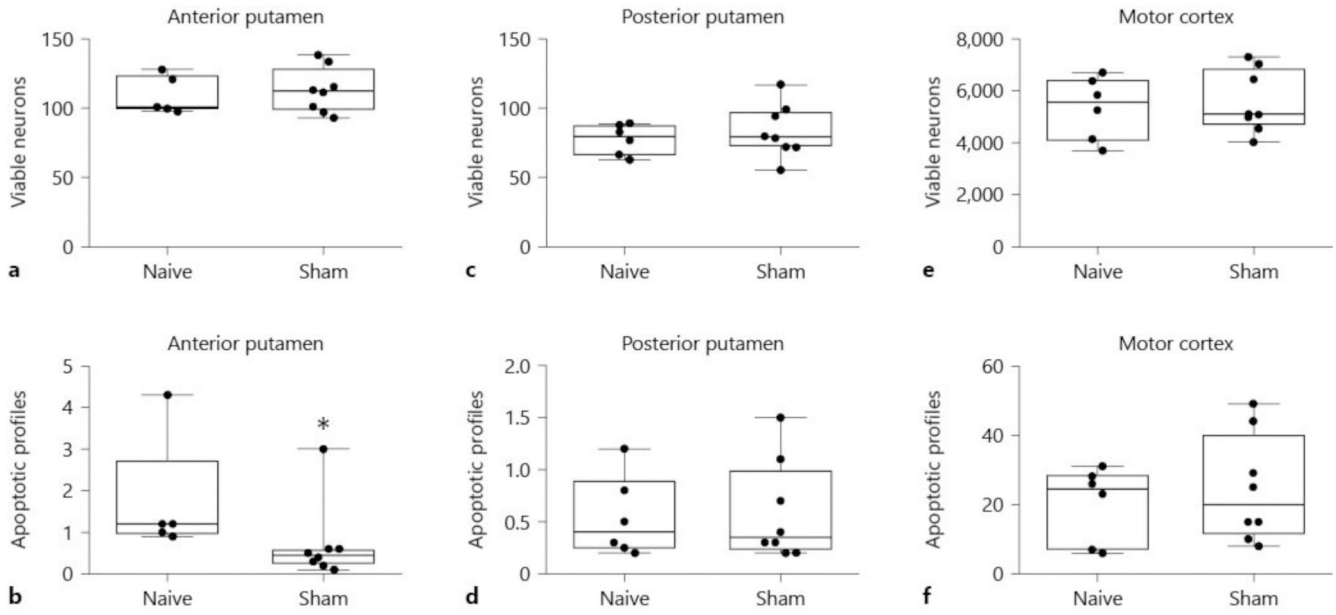

Fig. 4.

Viable neuron and apoptotic profile counts in anterior (**a**, **b**) and posterior (**c**, **d**) putamen and in motor cortex (**e**, **f**) of naïve and sham pigs. Counts were made on hematoxylin and eosin (H&E)-stained sections. The viable neuron counts were similar in naïve unanesthetized and sham normothermic piglets (**a**, $p = 0.693$ for anterior putamen; (**c**), $p = 0.311$ for posterior putamen). Naïve piglets had more apoptosis than did sham piglets, with a difference in medians of 0.75 apoptotic profiles per microscope field between groups in anterior putamen (**b**, * $p < 0.05$). Apoptotic profile counts did not differ in posterior putamen (**d**, $p = 1.00$). **e**, **f** Viable neuron and apoptotic profile counts did not differ in the motor cortex. Each circle represents 1 piglet. Box plots with IQRs and 5–95th percentile whiskers are shown.

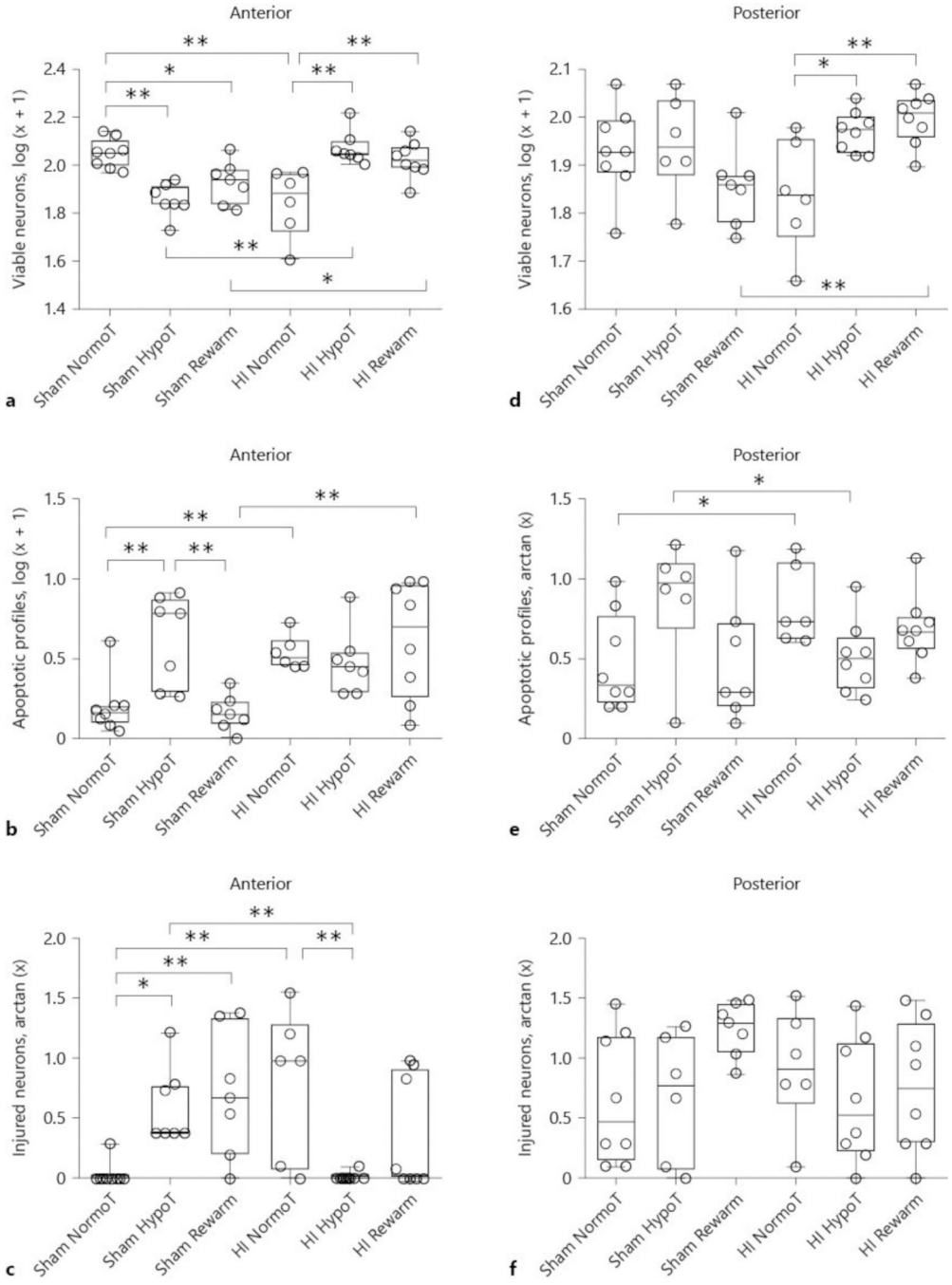

Fig. 5.

The effects of temperature and HI on viable neuron (**a**, **d**), apoptotic profile (**b**, **e**), and injured neuron (**c**, **f**) counts in anterior (**a**–**c**) and posterior (**d**–**f**) putamen on hematoxylin and eosin (H&E)-stained sections. **a** HI and temperature significantly interacted in their effect on the number of viable neurons ($p < 0.001$). * $p < 0.05$ and ** $p < 0.01$. **b** HI independently affected the number of apoptotic profiles ($p = 0.004$), and HI and temperature significantly interacted ($p = 0.003$). ** $p \leq 0.01$. **c** HI and temperature significantly interacted in their effect on injured neurons ($p < 0.001$). * $p < 0.05$ and ** $p < 0.01$. **d** In the

posterior putamen, HI and temperature significantly interacted in their effect on the number of viable neurons ($p = 0.003$). * $p < 0.05$ and ** $p < 0.01$. **e** HI and temperature interacted in their effect on apoptosis ($p = 0.008$) *$p < 0.05$. **f** HI and temperature did not affect the number of ischemic neurons in the posterior putamen ($p > 0.05$ for all comparisons). Each circle represents 1 piglet. Box plots with IQRs and 5–95th percentile whiskers are shown. Analyses were conducted by 2-way analysis of variance and post hoc pairwise comparisons with Holm-Sidak tests. NormoT, sustained normothermia; HypoT, sustained hypothermia; Rewarm, hypothermia followed by rewarming.

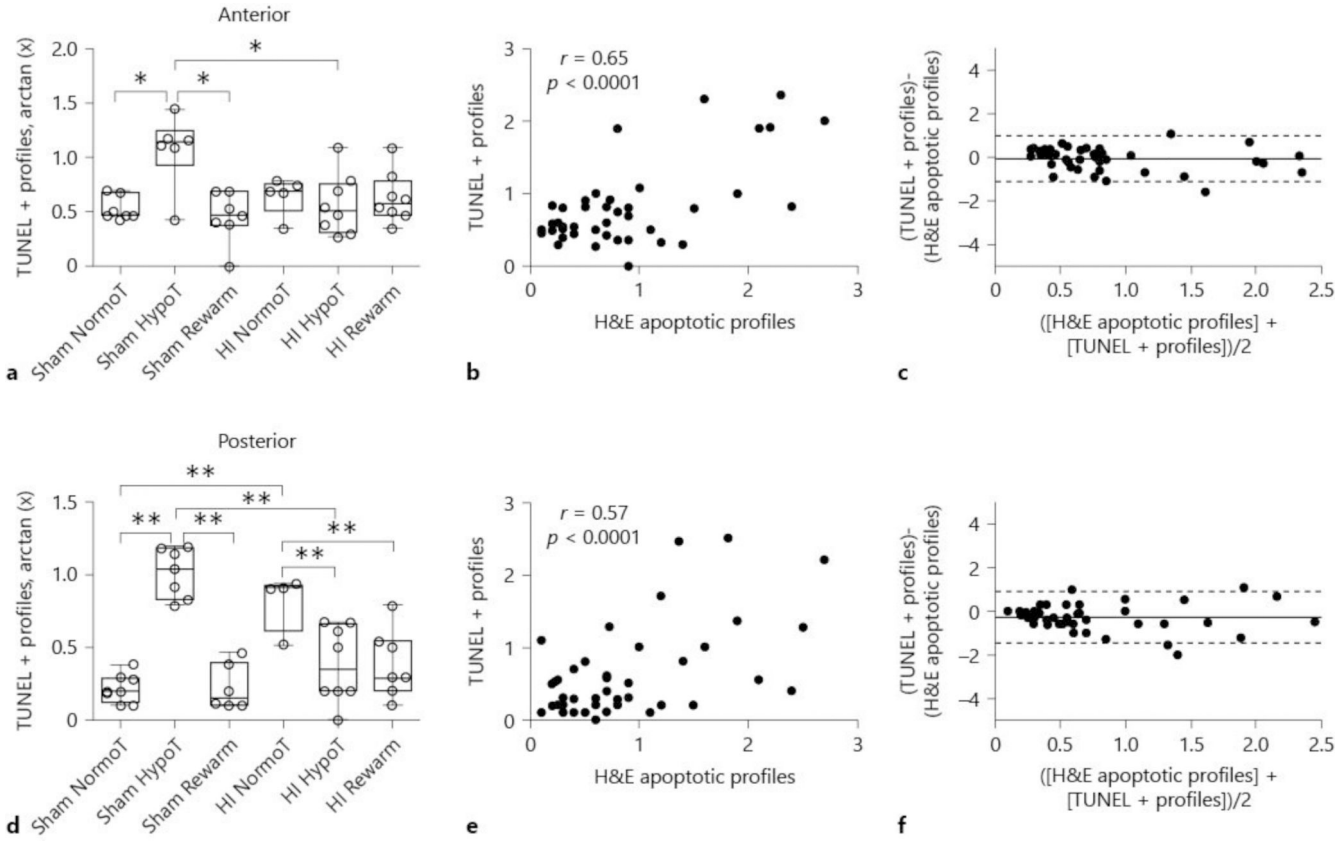

Fig. 6.

Terminal deoxynucleotidyl transferase dUTP nick-end labeling (TUNEL) staining to identify cell death in anterior putamen (**a**–**c**) and posterior putamen (**d**–**f**). **a** Temperature and HI interacted in their effect on the number of TUNEL+ cells ($p = 0.035$). * $p < 0.05$. **b** Interrater reliability analysis showed significant correlation in counting TUNEL+ cells and apoptotic profiles by hematoxylin and eosin (H&E) at the anterior level ($r = 0.65$, $p < 0.0001$). **c** Bland-Altman plot for TUNEL+ cells and apoptotic cells by H&E stain at the anterior level. Bias is shown by the solid line. The 95% limits of agreement are shown by dotted lines. Bias was near-zero with high agreement. **d** Temperature independently affected the number of TUNEL+ cells ($p < 0.001$), and HI and cooling had an interactive effect ($p < 0.001$) ** $p < 0.01$. **e** Interrater reliability analysis showed significant correlation in counting TUNEL+ cells and apoptotic profiles by H&E at the posterior level ($r = 0.57$, $p < 0.0001$). **f** Bland-Altman plot for TUNEL+ cells and apoptotic cells by H&E stain at the posterior level. Bias is shown by the solid line. The 95% limits of agreement are shown by dotted lines. Bias was near-zero with high agreement. Each circle represents 1 piglet. Data in (**a**, **b**) are graphed as box plots with IQRs and 5–95th percentile whiskers. Analyses in (**a**, **b**) were conducted by 2-way analysis of variance and post hoc pairwise comparisons with Holm-Sidak tests. NormoT, sustained normothermia; HypoT, sustained hypothermia; Rewarm, hypothermia followed by rewarming.

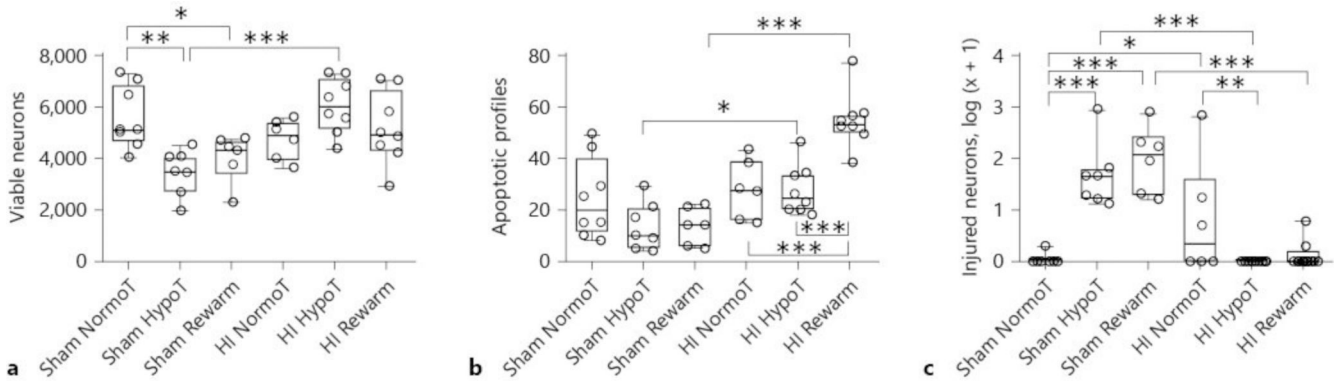

Fig. 7.

The effect of temperature and HI on viable neuron (**a**), apoptotic profile (**b**), and injured neuron (**c**) counts in the motor cortex. **a** HI had an independent ($p = 0.007$) and interactive effect with temperature ($p < 0.001$) on the number of viable neurons. * $p < 0.05$, ** $p < 0.01$, and *** $p < 0.001$. **b** HI ($p < 0.001$) and temperature ($p = 0.009$) independently and interactively ($p < 0.001$) affected the number of apoptotic profiles. * $p < 0.05$ and *** $p < 0.001$. **c** HI ($p < 0.001$) and temperature ($p = 0.014$) independently and interactively ($p < 0.001$) affected injured neuron counts. * $p < 0.05$, ** $p < 0.01$, *** $p < 0.001$. Each circle represents 1 piglet. Box plots with IQRs and 5–95th percentile whiskers are shown. Analyses were conducted by 2-way analysis of variance and posthoc pairwise comparisons with Holm-Sidak tests. NormoT, sustained normothermia; HypoT, sustained hypothermia; Rewarm, hypothermia followed by rewarming.

Table 1.

Primary antibodies used for Western blotting

Antibody	Dilution used	Manufacturer	Catalog number	Clonality	Role
Mouse anti-neuronal nuclei IgG	1:5,000	Millipore; Temecula, CA, USA	MAB377	Monoclonal	Specific neuronal marker
Goat anti-cleaved caspase 3 IgG	1:1,000	R&D Systems; Minneapolis, MD, USA	AF-605-NA	Polyclonal	Mediator of apoptosis
Rabbit anti-TNF-α IgG	1:100	Abcam; Cambridge, UK	Ab6671	Polyclonal	Marker of inflammation
Mouse anti-CD95 IgG	1:100	BD Transduction Laboratories; San Jose, CA, USA	610197	Monoclonal	Mediator of apoptosis
Rabbit anti-nitrotyrosine IgG	1:25,000	Millipore; Darmstadt, Germany	06–284	Polyclonal	Marker of inflammation
Rabbit anti-Iba1 IgG	1:1,000	Wako; Richmond, VA, USA	016–20001	Polyclonal	Microglia/macrophage marker
Mouse anti-HSP70 IgG	1:1,000	Abcam; Cambridge, UK	Ab2787	Monoclonal	Involved in unfolded protein response
Mouse anti-ERN1 IgG	1:500	Abgent; San Diego, CA, USA	AO1361a	Monoclonal	Involved in unfolded protein response
Rabbit anti-PERK IgG	1:1,000	Cell Signaling Technology; Danvers, MA, USA	3192	Monoclonal	Involved in unfolded protein response
Rabbit anti-pERN1 IgG	1:1,000	Novus Biologicals; Littleton, CO, USA	NB100–2323	Polyclonal	Involved in unfolded protein response

Table 2.

Cell profile counts in putamen at the anterior and posterior levels

Parameter/ Group	Anterior level								Posterior Level							
	n	H&E viable neurons	*n*	H&E ischemic neurons	*n*	H&E apoptotic profiles	*n*	TUNEL profiles	*n*	H&E viable neurons	*n*	H&E ischemic neurons	*n*	H&E apoptotic profiles	*n*	TUNEL profiles
Naive	*5*	100.8 (98.7– 124.2)	*5*	0 (0– 0.1)	*5*	1.2 (1.0– 2.8)	*6*	0.5 (0.3– 0.8)	*6*	79.4 (65.2– 87.8)	*6*	2.1 (0.2– 3.7)	*6*	0.4 (0.2– 0.9)	6	0.2 (0.1– 0.3)
Sham NormoT	8	112.2 (98.1– 129.0)	8	0 (0– 0)	8	0.5 (0.2– 0.6)	7	0.8 (0.5– 1.9)	8	84.3 (75.9– 97.8)	8	0.6 (0.2– 2.6	8	0.4 (0.2– 1.0)	8	0.2 (0.1– 0.3)
Sham HypoT	7	68.1 (67.8– 81.8)	7	0.4 (0.4– 1.0)	7	5.0 (0.9– 6.5)	6	1.4 (0.5– 2.3)	6	85.9 (74.5– 107.7)	6	1.0 (0.1– 2.6)	6	1.5 (0.9– 2.0)	7	1.7 (1.1– 2.5)
Sham Rewarm	7	86.3 (67.3– 96.0)	7	0.8 (0.2– 4.5)	7	0.4 (0.2– 0.7)	7	0.6 (0.4– 0.8)	7	71.0 (59.3– 75.2)	7	3.6 (1.7– 9.5)	7	0.3 (0.2– 0.9)	6	0.2 (0.1– 0.4)
HI NormoT	6	76.8 (52.4– 92.2)	6	1.5 (0.1– 12.4)	6	2.2 (1.8– 3.2)	5	0.8 (0.4– 1.2)	6	67.9 (55.3– 90.5)	6	1.4 (0.8– 7.6)	6	0.9 (0.7– 2.1)	4	1.3 (0.7– 1.3)
HI HypoT	7	111.9 (108.3– 127.6)	7	0 (0–0)	7	1.8 (0.9– 2.5)	8	0.5 (0.3– 0.8)	8	93.0 (83.9– 99.7)	8	0.6 (0.2– 2.3)	8	0.6 (0.3– 0.8)	8	0.4 (0.2– 0.8)
HI Rewarm	8	104.7 (96.6– 119.9)	8	0 (0– 1.4)	8	4.2 (0.8– 8.2)	6	0.7 (0.5– 1.0)	8	102.0 (88.9– 108.3)	8	1.0 (0.3– 4.2)	8	0.8 (0.6– 1.0)	7	0.3 (0.2– 0.6)

All data are presented as median (IQR).

H&E, hematoxylin and eosin; TUNEL, terminal deoxynucleotidyl transferase dUTP nick-end labeling; NormoT, sustained normothermia; HI, hypoxia-ischemia; HypoT, sustained hypothermia; Rewarm, hypothermia followed by rewarming.